

RESEARCH

Open Access



# NUAK1 promotes tumor metastasis through upregulating slug transcription in esophageal squamous cell carcinoma

Huiru Yang<sup>1</sup>, Zhen Wei<sup>1</sup>, Yifan Song<sup>3</sup>, Kexin Du<sup>3</sup>, Nannan Yin<sup>3</sup>, Hong Lu<sup>4</sup>, Bingbing Li<sup>4</sup>, Lili Hou<sup>1</sup>, Panfei Xing<sup>3</sup>, Liang Chen<sup>3\*</sup>, Chaojie Wang<sup>3\*</sup> and Songqiang Xie<sup>1,2\*</sup>

## Abstract

**Background** Metastasis is still a major cause of poor pathological outcome and prognosis in esophageal squamous cell carcinoma (ESCC) patients. NUAK1 has been reported highly expressed in many human cancers and is associated with the poor prognosis of cancer patients. However, the role of NUAK1 and its underlying signaling mechanism in ESCC metastasis remain unclear.

**Methods** Expression of NUAK1 in ESCC was detected by real-time quantitative RT-PCR (qRT-PCR), Western blotting and immunohistochemical staining. MTT, colony formation, wound-healing and transwell assays were used to determine the role NUAK1 in vitro. Metastasis was evaluated by use of an experimental pulmonary metastasis model in BALB/c-nu/nu mice. The mechanisms were assessed by using coimmunoprecipitation, immunofluorescence and dual-luciferase reporter gene experiments.

**Results** NUAK1 was highly expressed in ESCC tissues compared with the adjacent normal esophageal epithelial tissues. Moreover, the elevated expression of NUAK1 positively correlated with tumor invasion depth, lymph node metastasis, pathological TNM stage, and poor survival in ESCC patients. Further experiments showed that NUAK1 overexpression did not change the cell viability and colony formation of ESCC cells, while remarkably promoted the migration and invasion in vitro and experimental pulmonary metastasis in vivo. Mechanistically, NUAK1 enhanced the transcription level of Slug, which enhanced the migratory and invasive capability of ESCC cells. Consistently, silencing Slug almost completely diminished the migration and invasion of NUAK1-overexpressing ESCC cells. Further studies demonstrated that NUAK1 upregulated the transcription activity of Slug through activating the JNK/c-Jun pathway.

**Conclusion** These results demonstrated that NUAK1 promoted the metastasis of ESCC cells through activating JNK/c-Jun/Slug signaling, indicating NUAK1 is a promising therapeutic target for metastatic ESCC.

**Keywords** NUAK1, Slug, ESCC, Metastasis, EMT

\*Correspondence:

Liang Chen  
liang88chen@henu.edu.cn  
Chaojie Wang  
wcjsxq@henu.edu.cn  
Songqiang Xie  
xiesq@vip.henu.edu.cn

Full list of author information is available at the end of the article



© The Author(s) 2023. **Open Access** This article is licensed under a Creative Commons Attribution 4.0 International License, which permits use, sharing, adaptation, distribution and reproduction in any medium or format, as long as you give appropriate credit to the original author(s) and the source, provide a link to the Creative Commons licence, and indicate if changes were made. The images or other third party material in this article are included in the article's Creative Commons licence, unless indicated otherwise in a credit line to the material. If material is not included in the article's Creative Commons licence and your intended use is not permitted by statutory regulation or exceeds the permitted use, you will need to obtain permission directly from the copyright holder. To view a copy of this licence, visit <http://creativecommons.org/licenses/by/4.0/>. The Creative Commons Public Domain Dedication waiver (<http://creativecommons.org/publicdomain/zero/1.0/>) applies to the data made available in this article, unless otherwise stated in a credit line to the data.

## Background

Esophageal cancer is the seventh most frequently diagnosed cancer and the sixth leading cause of cancer death in the world, with an estimated 604,000 new cases and 544,000 deaths in 2020, according to the GLOBOCAN estimates of cancer incidence and mortality produced by the International Agency for Research on Cancer [1]. Esophageal squamous cell carcinoma (ESCC) is the most common histologic subtype of esophageal cancer in China, accounting for 90% of cases [2]. Although considerable advances achieved in diagnosis and multimodality therapies, the patients with ESCC often have a very poor prognosis, with the 5-year overall survival rate less than 15%, mainly due to the high incidences of tumor metastasis [3]. However, the precise mechanisms underlying the metastasis of ESCC remain unclear. Thus, it is imperative to identify potential molecular biomarkers for the diagnosis and treatment of metastatic ESCC.

Tumor metastasis is a sophisticated cascade process that includes acquisition of invasive and migratory abilities, breach of the basement membrane and detachment from the primary tumor, intrastation, survival in circulation flow, extravasation, adhesion, and colonization at the secondary site [4]. Epithelial mesenchymal transition (EMT), originally be described as an integral part of morphogenesis in embryonic development, has been shown to be a critical first step for the metastatic cascade process [5]. EMT is characterized by the loss of adherence junctions and apical-basal polarity, acquisition of mesenchymal phenotype, and the gain of migratory and invasive traits [6]. Undergoing EMT, cancer cells usually exhibit both morphological changes and molecular alterations, as demonstrated by lost expression of epithelial markers such as E-cadherin, ZO-1, and occludin, and increased expression of mesenchymal markers, including N-cadherin, vimentin, fibroblast-specific protein 1, and fibronectin [5]. In addition, EMT transcription factors (Snail, Slug, Zeb and Twist, etc.) are activated to orchestrate the EMT program [7]. However, mechanistic understanding of EMT in metastasis is still limited.

Novel (nu) kinase family 1 (NUAK1), also known as AMP-activated protein kinase (AMPK)-related protein kinase 5, is a serine/threonine kinase that has been identified as the fifth member of the AMPK catalytic subunit family [8]. Aberrant expression of NUAK1 has been observed in patients diagnosed with multiple cancer types including prostate cancer [9], nasopharyngeal carcinoma [10], pancreatic cancer [11] and colorectal cancer [12]. The high NUAK1 expression positively correlated with tumor stage, invasiveness, poor differentiation, lymph node metastasis [13] and the reduced overall survival of cancer patients [11]. The pro-metastatic function of NUAK1 was first uncovered in pancreatic cancer and

colon cancer, which was supported by the observation that ectopic overexpression of NUAK1 in human pancreatic cancer cell line PANC-1 and human colon cancer cell line DLD-1 induced a dramatic increase in migration and invasion activity in vitro and metastasis in vivo [14]. Subsequently, the pro-metastatic function of NUAK1 has also been demonstrated in breast cancer [15], head and neck cancer [16] and hepatocellular carcinoma [17]. These findings indicated that NUAK1 is a potential target for metastatic malignancies. Indeed, knockdown of NUAK1 remarkably suppressed the tumor cell invasion and metastasis in gastric cancer [18], nasopharyngeal carcinoma [19] and ovarian cancer [20]. However, the expression and potential role of NUAK1 in ESCC has never been investigated.

In this study, both gain- and loss-of-function studies showed that NUAK1 did not influence the cellular proliferation and colony formation, while remarkably promoted the migration, invasion and metastasis in ESCC. We further demonstrated that NUAK1 promoted the transcription activity of Slug through activating the JNK/c-Jun pathway. Collectively, our findings highlight the oncogenic role of NUAK1 in promoting ESCC cell migration, invasion and metastasis through activating JNK/c-Jun/Slug signaling, implicating that NUAK1 is a potential therapeutic target for the metastatic ESCC.

## Materials and methods

### Clinical samples

All ESCC tissues and the paired adjacent normal tissues used in this study were obtained from January 2016 to November 2022 in the Huaihe Hospital of Henan University. All the patients enrolled in the research haven't received radiation or chemotherapy treatment before surgery. All processes were approved by the Ethics Committees of Henan University (Kaifeng, China) and written informed consent was obtained from each patient prior to sample collection according to the principles of Helsinki Declaration. The immunohistochemistry (IHC) staining was performed as described previously [21]. The tumor tissues were stained with anti-NUAK1 antibody (1:100) and scored. The staining intensity was classified into four degrees (0, no staining; 1, low intensity; 2, moderate intensity; and 3, strong intensity). The final IHC staining scores = (score of the staining intensity) × (the proportion of positively stained cells) [21].

### Cell lines and cell culture

The human ESCC cell lines EC9706, EC109, KYSE70, KYSE510, KYSE150, and KYSE30, and one normal esophageal epithelial cell line (Het-1A) were cultured as our previously described [22]. All cells were maintained in a humidified atmosphere (5% CO<sub>2</sub>) at 37 °C and

were recently tested for STR profiling and mycoplasma contamination.

#### Antibodies and reagents

The anti-NUAK1 antibody (22723-1-AP) and anti- $\beta$ -actin antibody (23660-1-AP) were purchased from ProteinTech (Chicago, IL, USA); the anti-E-cadherin (#14472), anti-Vimentin (#46173), anti-N-cadherin antibody (#13116), TWIST1 (#90445), ZEB1 (#83243), Snail (#3879), Slug (#9585), p-c-Jun (S73) (#3270), c-Jun (#9165), p-JNK (T183/Y185) (#4668), JNK (#9252), p-Erk1/2 (T202/Y204) (#4370), Erk1/2 (#4695), p-p38 (T180/Y182) (#54470) and p38 (#9212) were purchased from Cell Signaling Technology (CST, Danvers, MA, USA). SP600125 (HY-12,041), JNK-IN-8 (HY-13,319) and puromycin dihydrochloride (HY-B1743A) were purchased from MCE (NJ, USA).

#### Quantitative real-time polymerase chain reaction (qRT-PCR)

For this experiment, RNA extraction was performed as previously described [21]. Briefly, total RNA was extracted from cultured cell lines or frozen clinical tissues using Trizol reagent (Invitrogen, USA), and 1  $\mu$ g of the total RNA was reverse transcribed with a Revert Aid First Strand cDNA Synthesis Kit (#K1622, Thermo, USA) according to the manufacturer's protocol. qRT-PCR was performed with LightCycler 480 SYBR Green I Master (Roche, Basel, Switzerland) using the LightCycler<sup>®</sup> 480 Instrument II (Roche Diagnostics AG, Rotkreuz, Switzerland). The sequences of the primers used for amplifying NUAK1, Slug and GAPDH are listed in Additional file 1: Table S1. Relative mRNA expression was calculated using the  $2^{-\Delta\Delta C_t}$  method and normalized to those of the internal control gene GAPDH.

#### Western blot analysis

Total protein was extracted from cultured cells and analyzed as previously described [22]. Briefly, the whole cell lysates were prepared in RIPA buffer containing 1 $\times$  protease inhibitor cocktail (Roche, Indianapolis, IN), 1 mM phenylmethylsulfonyl fluoride, 10 mM  $\beta$ -glycerophosphate and 10 mM NaF. The concentration of total protein was quantified by using Pierce<sup>™</sup> BCA Protein Assay Kit (#23250, Thermo, USA). A total of 30  $\mu$ g of protein extracts were loaded to 10% sodium dodecyl sulfate-polyacrylamide gel electrophoresis (SDS-PAGE) and transferred to PVDF membranes (Millipore, USA). After blocking with 5% dried skimmed milk for 1 h at room temperature, the membrane was incubated with the primary antibodies overnight at 4 °C and then with HRP conjugated secondary antibodies (Promega, USA) for 1 h at room temperature, Protein bands were detected

using enhanced chemiluminescence (ECL) detection reagent (Beyotime, Shanghai, China) on a FluorChem M system (Protein Simple, USA).

#### Co-immunoprecipitation (Co-IP) assay

This experiment was performed using the Immunoprecipitation Kit with Protein A Magnetic Beads (#P2175S, Beyotime, Shanghai, China) according to the manufacturer's instructions. Briefly, cells were harvested in lysis buffer containing protease inhibitor cocktail and phosphatase inhibitor cocktail A (#P1081, Beyotime, Shanghai, China), incubated for 30 min on ice and centrifuged at 12,000 $\times$ g at 4 °C for 10 min. Cell lysates were immunoprecipitated with antibodies against NUAK1 and JNK or negative control IgG and protein A magnetic bead overnight with rotation. After being washed three times with lysis buffer, these beads were resuspended in 50  $\mu$ L SDS-PAGE sample loading buffer, denaturalized at 100 °C for 5 min and subjected to Western blot analysis.

#### Plasmid construction and lentivirus Infection

The constructs encoding full-length human NUAK1, Slug and c-Jun cDNA were subcloned into the pLVX-IRES-neo vector. The pLVX-IRES-neo empty vector was used as negative control. Non-targeting (mock) siRNA (#sc-37007) and siRNA oligoduplexes against c-Jun (#sc-29223) were obtained from Santa Cruz Biotechnology (Santa Cruz, CA, USA). Scramble (pLKO.1-puro-Non-target shRNA), specific target shRNAs against human NUAK1 or Slug were purchased from Sigma-Aldrich (Shanghai, China). Cells were transfected with siRNA duplexes using Lipofectamine<sup>™</sup> RNAiMAX Transfection Reagent (#13778100, Thermo, USA) according to the manufacturer's instructions. The transfection of overexpressing plasmids and shRNA constructs was carried out using Lipofectamine<sup>™</sup> 3000 Transfection Reagent (#L3000015, Thermo, USA). For lentivirus production, the indicated lenti-vectors and the packaging plasmids (pCMV-dR8.2 dvpr and pCMV-VSV-G) were cotransfected into 293T cells. The culture medium containing mature lentivirus particles was collected and purified with 0.45- $\mu$ m filters at 48 h after transfection. Then the indicated lentivirus and polybrene (8  $\mu$ g/mL) were added to ESCC cells, after infection for 24 h, cells were selected with puromycin (1.5  $\mu$ g/mL) or G418 (800  $\mu$ g/mL) for 2 weeks to establish stable cell populations.

#### MTT assay

The MTT assay was conducted to examine the effects of NUAK1 overexpression and knockdown on the viability of ESCC cells as described previously [22]. Briefly, cells were seeding into 96-well culture plates at the density of 1000 cells/well and assessed at five time points (on days

1, 2, 3, 4, and 5). Twenty microliters of MTT (Sigma-Aldrich, USA) reagent (5 mg/mL) was added into each well, and the plates were incubated at 37 °C for another 4 h. After discarding the supernatant, one hundred microliters of DMSO was added to dissolve the formed formazan crystals. Then the optical density (OD) value was measured by a spectrophotometric plate reader (Synergy HT; BioTek, Winooski, VT, USA) at 570 nm. Each group was comprised of four duplicated wells, and the assay was performed five times independently.

#### **Foci formation and soft agar assays**

For foci formation assay, cells (500/well) stably transfected with NUA1 or NUA1 shRNA were seeded into 24-well plates and cultured for 14 days. Colonies composing containing  $\geq 50$  cells were fixed and stained with 0.1% crystal violet in 20% methanol for 20 min and counted using an inverted microscope (Olympus, Japan). For soft agar assay, cells (2000/well) mixed with 0.4% Bacto-agar (#A5306, Sigma-Aldrich, Shanghai, China) were plated on a bottom layer of solidified 0.8% agar in a 24-well plate. Two weeks later, the surviving colonies composing more than 50 cells were determined by microscope counting.

#### **Immunofluorescence**

Briefly, cells were washed with PBS, fixed with 4% paraformaldehyde for 20 min, permeabilized with 0.5% Triton X-100 for 15 min and blocked with 3% bovine serum albumin in PBS for 1 h at room temperature. Cells were then incubated overnight with primary antibodies: E-cadherin (#14472, 1:200, CST) and Vimentin (#46173, 1:100, CST). After washing with PBS, cells were incubated with anti-mouse Alexa Fluor 594 antibody (#8890, 1:1000, CST) or anti-rabbit Alexa Fluor 488 antibody (#4412, 1:1000, CST) at room temperature. After washing thrice with PBS, the cells were by incubation for 5 min with DAPI (#4083, 0.5  $\mu\text{g/mL}$ , CST) to label the nuclei. Images were captured using a confocal scanning microscope (Leica TCS SP8, Germany).

#### **Wound-healing assay**

Cells were seeded in 6-well plates at a density of  $5 \times 10^5$  cells/well and cultured until 80–90% confluence. A 10  $\mu\text{L}$  sterile pipette tip was used to introduce a straight scratch simulating a wound, the wells were washed with PBS to remove the floating cells, and the medium was then replaced with serum-free culture medium. Images were captured at 0 h, 24 and 48 h after scratching using an inverted microscope.

#### **Cell migration assay and invasion assays**

This experiment was performed using chambers with polyethylene terephthalate membranes (8  $\mu\text{m}$  pore size) (BD Biosciences, USA) as previously described [22]. Briefly, cells were suspended in serum-free RPMI 1640 medium and added to the upper chamber, which was coated without (migration assay) or with (invasion assay) the Matrigel mix (BD Biosciences, USA). Culture medium supplemented with 10% FBS was placed into the lower chamber as a chemo-attractant. After 24 h of incubation, the migrated or invaded cells on the bottom of the membrane were stained with 0.1% Crystal Violet. The total number of cells was counted from six random fields using an inverted microscope (Olympus, Japan). All experiments were performed in duplicate and repeated five times.

#### **Dual-luciferase reporter gene assay**

Cells were plated in 24-well plates and cultured for overnight. The cells were then cotransfected with the appropriate pGL3-Slug promoter-luciferase plasmid or pGL3-luciferase control plasmid, together with the renilla luciferase control reporter using the Lipofectamine 3000 kit (#L3000015, Thermo, USA). Forty-eight hours later, the luciferase activities in the cell lysates were measured using the Dual-Luciferase<sup>®</sup> Reporter Assay System (#E1910, Promega, USA) in accordance with the manufacturer's instructions and normalized with renilla luciferase activity. All of the experiments were performed in five times.

#### **In vivo tumor metastasis**

All animal experiments were approved by the Henan University Institutional Animal Care and Use Committee. Five-week-old male BALB/c-nu/nu mice purchased from Vital River (Beijing, China) were housed in specific pathogen-free (SPF) conditions in a laboratory animal facility with controlled temperature ( $20 \pm 2$  °C), humidity (40–50%) and a lighting cycle of 12 h darkness/12 h light.

For the in vivo metastasis assays,  $2 \times 10^6$  NUA1-overexpressing EC109 cells or NUA1-knockdown KYSE30 cells and control cells were separately injected into the lateral tail veins of nude mice (6 per group). After 8 weeks, the mice were sacrificed with isoflurane, and their lungs were harvested at necropsy and fixed in Bouin's solution. The numbers of metastatic colonies on the lung surface of each mouse were carefully counted, and histological evidence of the lung tissues was further examined by hematoxylin and eosin (H&E) or IHC staining.

### Database analysis

the mRNA level of NUA1 in TCGA ESCC samples was analyzed using UALCAN database (<http://ualcan.path.uab.edu/index.html>). The NUA1 transcriptome data downloaded from Gene Expression Omnibus (GEO) database (Accession Number GSE23400, GSE44021 and GSE53625) (<https://www.ncbi.nlm.nih.gov/geo/>) was analyzed using the limma packages for GEO data by R software.

### Statistical analysis

The data are presented as the mean  $\pm$  the standard deviation (SD) of at least three independent experiments. The statistical analysis was performed using SPSS software version 22.0 (Chicago, IL, USA) and all graphs were performed by GraphPad Prism software 7.0 (San Diego, CA, USA). Student's *t*-test or paired *t*-test was used to compare the differences between two groups. We compared 3 or more groups with one-way ANOVA with Tukey's post hoc test, the overall *F* test was significant ( $P < 0.05$ ), and there was no significant variance in homogeneity. Survival curves were constructed by the Kaplan–Meier method, and a log-rank test was used for comparison. All statistical tests were two-sided, and a *P* value of less than 0.05 was regarded as statistically significant.

## Results

### NUAK1 is highly elevated in ESCC

To determine the expression of NUA1 in ESCC, we first analyzed the mRNA level of NUA1 using TCGA samples from UALCAN database (<http://ualcan.path.uab.edu/index.html>), the results showed that NUA1 was highly expressed in ESCC specimens ( $n = 95$ ) compared to that in esophageal adenocarcinoma (EAC) ( $n = 89$ ) and the adjacent normal tissues ( $n = 11$ ) (Fig. 1A). We further analyzed the expression of NUA1 with three GEO datasets (GSE23400, GSE44021 and GSE53625). As shown in Fig. 1B, the mRNA level of NUA1 was much higher in ESCC tissues compared with the adjacent normal counterparts. To verify the bioinformatic analysis results, we examined a set of ESCC and paired adjacent normal tissues, confirming that NUA1 mRNA levels were upregulated in cancerous tissues, compared to the paired

adjacent normal counterparts (Fig. 1C). To explore the protein expression and localization of NUA1 in ESCC tissues, we performed IHC staining on ESCC sections. As illustrated Fig. 1D, NUA1 was highly expressed in ESCC tissues compared with that in adjacent esophageal epithelial tissues and it is mainly expressed in the cytoplasm and nucleus of ESCC cells. Further analysis showed that the elevated NUA1 expression was positively correlated with T stage (primary tumor invasion depth), N stage (lymph node metastasis) and pathological TNM stage but has no correlation with age, gender, tumor location or differentiation (Fig. 1E–G and Additional file 1: Table S2). Kaplan–Meier analysis revealed that high NUA1 expression in ESCC patients was positively associated with reduced overall survival (Fig. 1H). Consistently, the positive correlation between NUA1 expression and poor prognosis was further confirmed in TCGA ESCC samples (Fig. 1I). Taken together, these results indicate that NUA1 is aberrantly expressed in ESCC tissues and probably play an oncogenic role in ESCC progression and metastasis.

### NUAK1 does not affect the growth of ESCC cells

To further investigate the potential role of NUA1 in regulating the malignant process of ESCC, we first detected the mRNA and protein levels of NUA1 in seven ESCC cell lines (EC109, EC9706, TE-1, KYSE30, KYSE70, KYSE150 and KYSE510) and an immortalized esophageal epithelial cell line (Het-1 A). The results showed that elevated NUA1 expression was observed in all tested ESCC cell lines, compared with the immortalized Het-1 A esophageal epithelial cell line (Fig. 2A, B). We used lentiviruses to overexpress NUA1 in EC109 and KYSE510 cells, which endogenously express a lower level of NUA1 among the tested ESCC cells. The transfection efficiency of NUA1 was confirmed by Western blot analysis (Fig. 2C). MTT cell growth assay showed that ectopic expression of NUA1 did not affect the cell viabilities of EC109 and KYSE510 cells (Fig. 2D). We further examined whether overexpression of NUA1 promotes the colony formation using foci formation assay and soft agar assay. However, no significant differences

(See figure on next page.)

**Fig. 1** NUA1 is highly expressed in ESCC. **A** The mRNA level of NUA1 was analyzed in normal and cancerous tissues from the TCGA cohort. **B** Data from the GEO database showed that NUA1 was upregulated in ESCC tissues compared to the adjacent normal counterparts. **C** qRT-PCR analysis of the levels of NUA1 mRNA in 19 pairs of ESCC tumor and matched normal tissues. **D** IHC staining for NUA1 was performed in 116 pairs of ESCC tissues and adjacent normal tissues. Representative images (left panel) and IHC scores (right panel) are shown (scale bar, 100  $\mu$ m). *P* value was calculated by paired *t*-test (for **A–D**). **E–G** The NUA1 staining score for T stage (**E**), N stage (**E**) and pathological TNM stage (**E**) in ESCC. *P* value was calculated by Student's *t*-test (for **E–G**). **H** Kaplan–Meier analysis revealed that high NUA1 expression predicted poor prognosis in ESCC. **I** Survival analysis of TCGA patients from whom the ESCC samples were obtained based on the NUA1 expression level. *P* value was calculated by the log-rank test (for **H** and **I**). Error bars denote mean  $\pm$  SD. \* $P < 0.05$ ; \*\* $P < 0.01$ ; \*\*\* $P < 0.001$

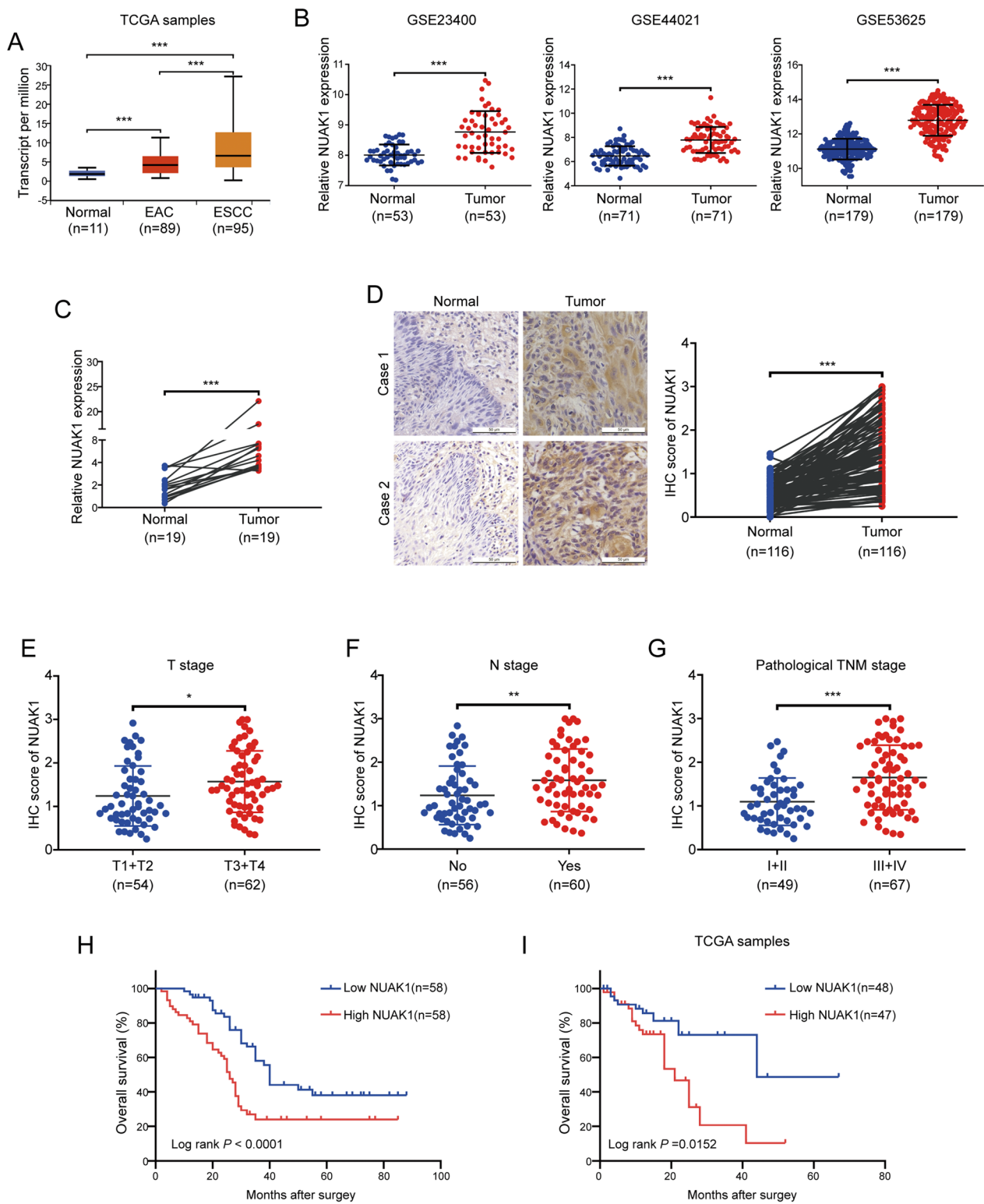


**Fig. 1** (See legend on previous page.)

were observed between NUA1-overexpressing and control cells (Fig. 2D, E). Next, we determined whether knocking down NUA1 suppresses the tumorigenic ability of ESCC cells. Two pairs of small hairpin RNAs (shRNAs) against NUA1 were used to dramatically reduce endogenous NUA1 expression in KYSE30 and KYSE150 cells, which endogenously express a high level of NUA1 (Fig. 2G). The results revealed that the cell viability and colony formation of KYSE30 and KYSE150 cells was just marginally inhibited by NUA1 shRNA, compared with the control group (Fig. 2H–J). Collectively, these data together suggest that NUA1 does not influence the growth of ESCC cells.

#### NUAK1 promotes ESCC cell migration and invasion

Subsequently, we sought to determine the potential role of NUA1 on the migration and invasion of ESCC cells. Wound-healing scratch assay showed that ectopic overexpression of NUA1 greatly enhanced the wound-closure capability of EC109 and KYSE510 cells (Fig. 3A). Similarly, the NUA1-overexpressing ESCC cells showed a significantly increased migration ability using transwell migration assay (Fig. 3B). Assessed by transwell invasion assays, overexpression of NUA1 dramatically increased the number of invaded ESCC cells (Fig. 3C). Considering overexpression of NUA1 promoted the migration and invasion of ESCC cells, we then sought to examine whether silencing NUA1 attenuates these malignant behaviors. As shown in Fig. 3D, knockdown of NUA1 significantly abolished the motility of KYSE30 and KYSE150 cells. Consistent with this result, transwell migration assay also showed that the NUA1-knockdown ESCC cells showed a significantly decreased migration ability, compared with those cells with shNC transfection (Fig. 3E). In addition, the number of tumor cells invaded through Matrigel were decreased in both tested NUA1-depleted ESCC cells (Fig. 3F). Collectively, these data demonstrate that NUA1 overexpression promotes the migratory and invasive capability of ESCC cells.

#### NUAK1 promotes slug-mediated EMT in ESCC cells

Increasing reports have shown that EMT is associated with cancer migration, invasion and metastasis [5, 23, 24]. Because NUA1-overexpressing cells exhibited a more fibroblast-like mesenchymal features compared with their control cells, which displayed epithelial-like phenotype (Fig. 4A). In addition, we also noticed that the morphology of stable NUA1-knockdown cells has been changed from the spindle-like and fibroblastic phenotype (mesenchymal feature) into the tight cell-to-cell adhesion (epithelial-like phenotype) (Fig. 4A), suggesting NUA1 promoted EMT in ESCC cells. We then decided to detect whether NUA1 influence the EMT-related proteins in NUA1-overexpressing and knockdown cells using Western blot analysis. As shown in Fig. 4B and Additional file 1: Fig. S1A, we found that ectopic overexpression of NUA1 inhibited the expression of E-cadherin, while enhanced the expression of the mesenchymal markers, N-cadherin and Vimentin. In contrast, silencing NUA1 inhibited the expression of the mesenchymal markers, N-cadherin and Vimentin, while reducing E-cadherin expression in both tested NUA1-knockdown cells (Fig. 4B and Additional file 1: Fig. S1A). Moreover, immunofluorescence assay also showed that ectopic expression of NUA1 downregulated E-cadherin expression, while upregulating Vimentin expression in EC109 and KYSE510 cells (Fig. 4C). Considering the crucial role of EMT-related transcription factors (Twist, ZEB1, Snail and Slug) for EMT, we then detected whether NUA1 altered their expression using immunoblotting analysis. Strikingly, only Slug was remarkably increased in NUA1-overexpressing cells and was diminished in NUA1-knockdown cells (Fig. 4D and Additional file 1: Fig. S1B). To further investigate the role of Slug in NUA1-mediated EMT, we used two pairs of small hairpin RNAs (shRNAs) to dramatically reduce endogenous Slug expression in NUA1-overexpressing EC109 cells (Fig. 4E and Additional file 1: Fig. S1C). As expected, silencing Slug remarkably rescued the expression of E-cadherin, while diminishing the levels of N-cadherin and Vimentin induced by NUA1 overexpression (Fig. 4F and Additional file 1: Fig. S1D). On the other

(See figure on next page.)

**Fig. 2** NUA1 does not influence the tumor cell growth in ESCC cells. **A, B** The expression of NUA1 in ESCC cells at mRNA and protein levels were detected by qRT-PCR (**A**) and Western blotting (**B**), respectively. *P* value was calculated by one-way ANOVA with post hoc intergroup comparison by the Tukey's test. **C** Western blot analysis was performed to detect the level of NUA1 in EC109 and KYSE510 cells stably expressing NUA1. Quantification of indicated protein levels of *n* = 3 independent biological experiments (low panel). **D–F** The effects of NUA1 overexpression on ESCC cell growth were assessed by MTT assay (**D**), foci formation assay (**E**) and soft agar assay (**F**). *P* value was calculated by Student's *t*-test (for **C–F**). **G** KYSE30 and KYSE150 cells stably expressing shNC or NUA1 shRNA as indicated were analyzed by Western blotting. Quantification of indicated protein levels of *n* = 3 independent biological experiments (low panel). **H–J** The effects of NUA1 knockdown on ESCC cell growth were assessed by MTT assay (**H**), foci formation assay (**I**) and soft agar assay (**J**). *P* value was calculated by one-way ANOVA with post hoc intergroup comparison by the Tukey's test (for **G–J**). Error bars denote mean ± SD. \**P* < 0.05; \*\**P* < 0.01; \*\*\**P* < 0.001

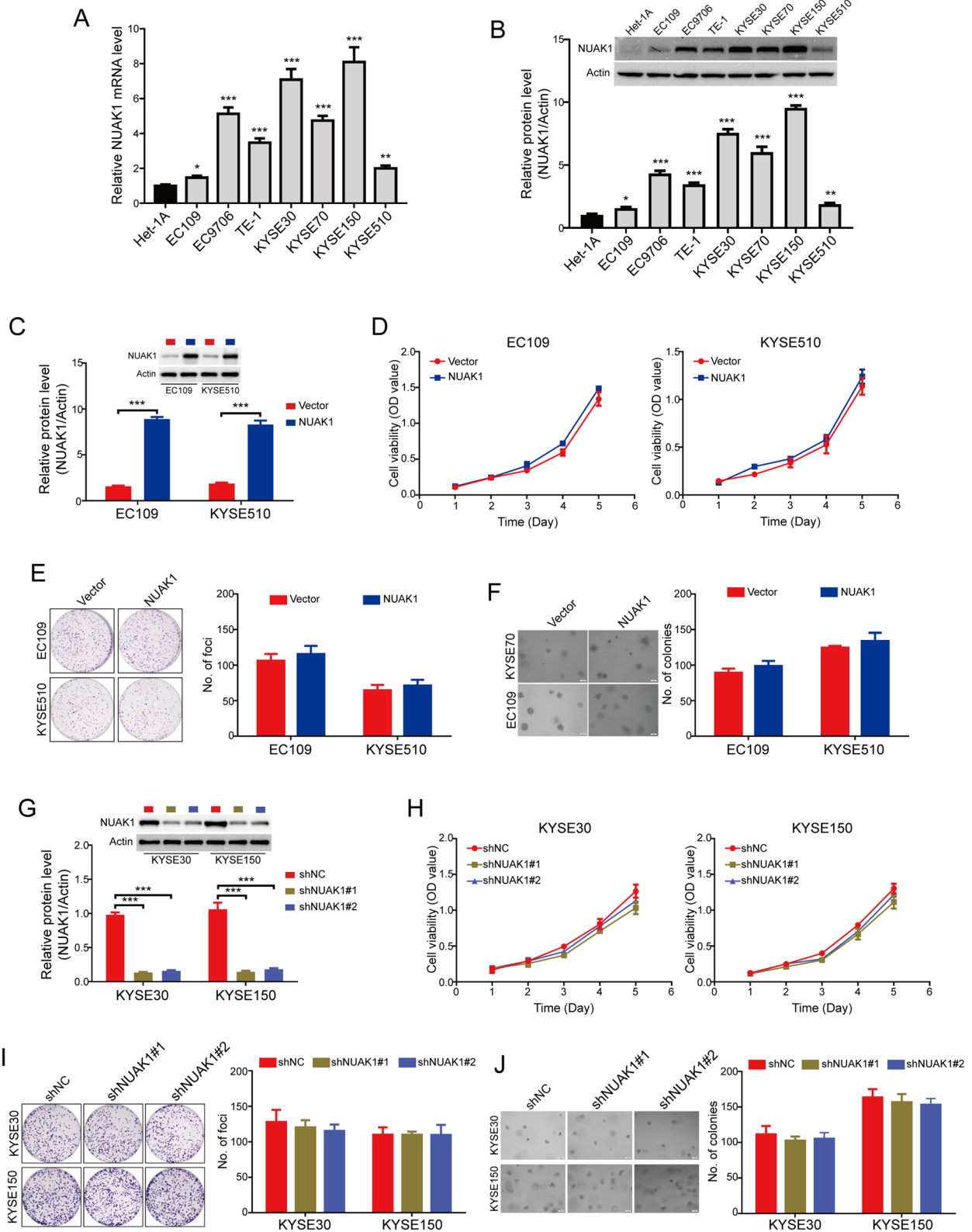


**Fig. 2** (See legend on previous page.)

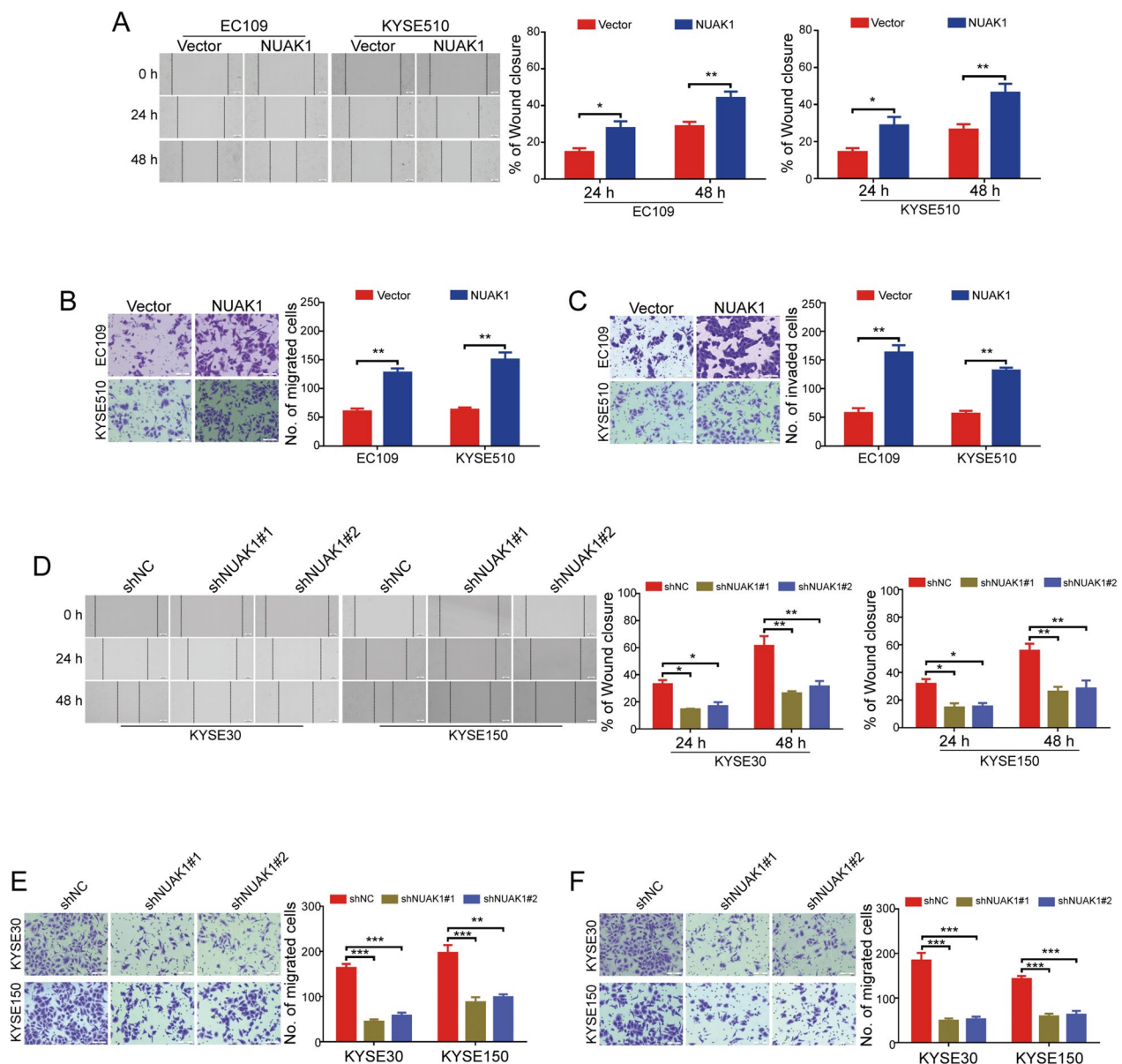


**Fig. 3** NUA1 promotes the migration and invasion of ESCC cells. **A–C** The effects of NUA1 overexpression on ESCC cell migration and invasion were assessed by wound healing assay (**A**), transwell migration (**B**), and invasion assay (**C**). *P* value was calculated by Student’s *t*-test. **D–F** The effects of NUA1 knockdown on ESCC cell migration and invasion were assessed by wound healing assay (**D**), transwell migration (**E**), and invasion assay (**F**). *P* value was calculated by one-way ANOVA with post hoc intergroup comparison by the Tukey’s test. Error bars denote mean ± SD. \**P* < 0.05; \*\**P* < 0.01; \*\*\**P* < 0.001

(See figure on next page.)

**Fig. 4** NUA1 promotes ESCC cell migration and invasion via Slug-mediated EMT. **A** The effects of NUA1 overexpression and knockdown on the morphological changes of ESCC cells were shown. **B** The effects of NUA1 overexpression and knockdown on the protein levels of E-cadherin, N-cadherin and Vimentin were measured by Western blotting. **C** The effects of NUA1 overexpression on E-cadherin and Vimentin were analyzed by immunofluorescence assay. **D** Relative expressions of the indicated molecules were detected by Western blotting. **E** Western blot analyses of the levels of Slug, E-cadherin, N-cadherin and Vimentin in NUA1-overexpressing EC109 cells treated with Slug shRNA. **F** Transwell assay was used to detect the migration (left panel) and invasion (right panel) in NUA1-overexpressing EC109 cells treated with Slug shRNA. **G** Western blot analyses of the levels of Slug, E-cadherin, N-cadherin and Vimentin in NUA1-knockdown KYSE30 cells treated with Slug and control plasmids. **H** Transwell assay was used to detect the migration (left panel) and invasion (right panel) in NUA1-knockdown KYSE30 cells treated with Slug and control plasmids. *P* value was calculated by one-way ANOVA with post hoc intergroup comparison by the Tukey’s test. Error bars denote mean ± SD. \**P* < 0.05; \*\**P* < 0.01; \*\*\**P* < 0.001

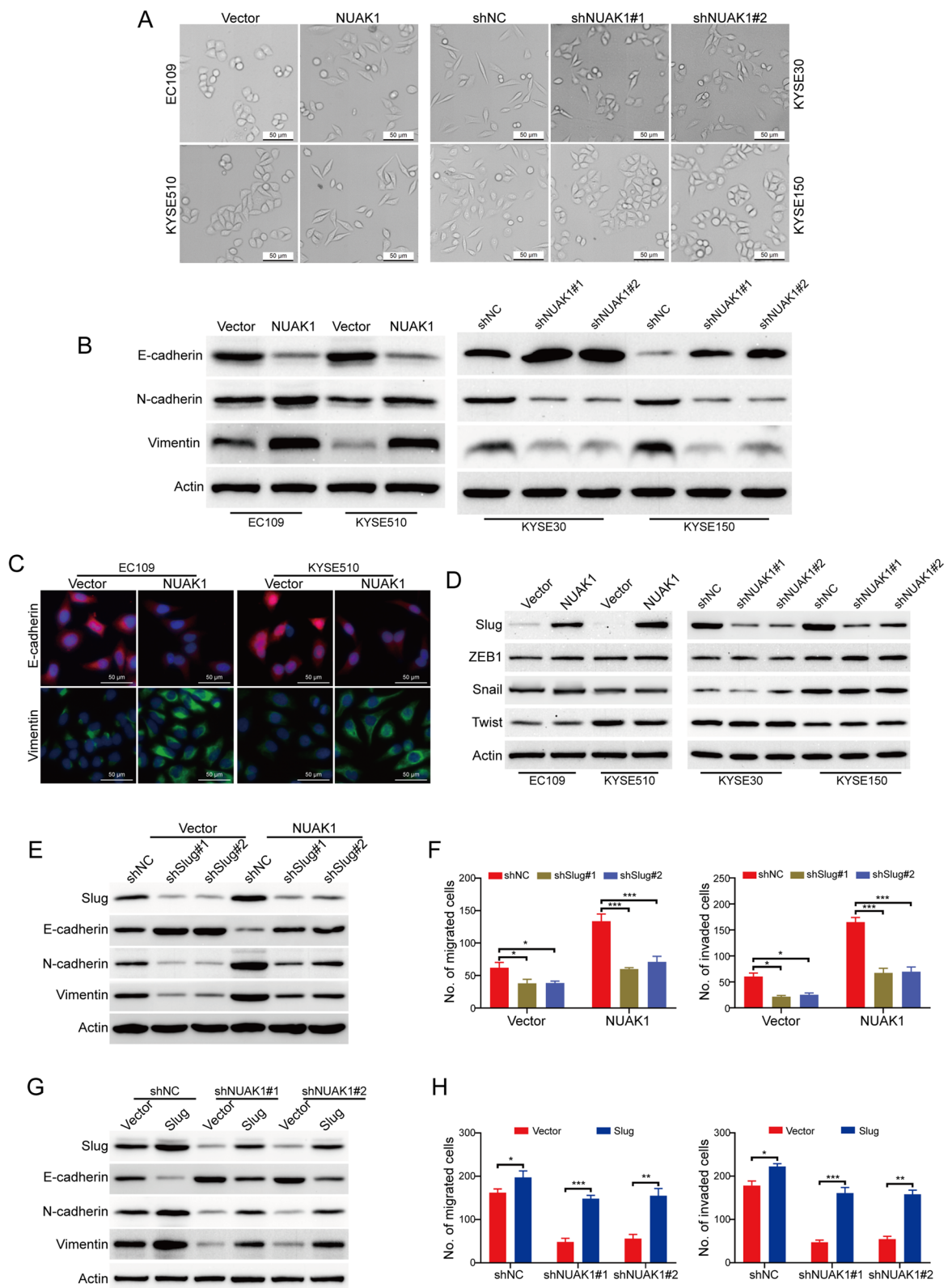


**Fig. 4** (See legend on previous page.)

hand, Slug was transiently transfected into the NUAK1-silenced KYSE30 cells, and the migratory and invasive abilities were almost rescued to the original levels in the KYSE30 cells (Fig. 4G, H). Taken together, our results indicate that NUAK1 promotes migration and invasion via Slug-mediated EMT in ESCC cells.

#### c-Jun is crucial for slug transcription induced by NUAK1 in ESCC cells

To explore how NUAK1 promotes Slug expression, the experiment of qRT-PCR was carried out to examine the mRNA level of Slug in ESCC cells. The results showed that the transcription of Slug was upregulated in NUAK1-overexpressing EC109 and KYSE510 cells, while was downregulated in NUAK1-depleted KYSE30 and KYSE150 cells (Fig. 5A). Considering that c-Jun has been identified as a critical transcription factor to regulate Slug expression through the AP1 site in the Slug promoter [25]. To determine whether c-Jun participates in Slug transcription induced by NUAK1 in ESCC cells, we constructed a slug promoter reporter plasmid by linking the slug promoter to a luciferase gene and transfected this plasmid into the tested ESCC cells. Assaying luciferase activity showed that slug promoter activity was significantly enhanced by NUAK1 in NUAK1-overexpressing EC109 and KYSE510 cells, while was inhibited by NUAK1 shRNA in NUAK1-depleted KYSE30 and KYSE150 cells (Fig. 5B). Moreover, silencing c-Jun by siRNA duplexes against c-Jun drastically diminished the expression of Slug in NUAK1-overexpressing EC109 cells (Fig. 5C). Consistently, luciferase reporter assay also showed that knocking down c-Jun greatly abrogated the Slug promoter activity induced by NUAK1 (Fig. 5D). These results suggest that c-Jun is crucial for NUAK1-induced Slug transcription in ESCC. To further determine whether c-Jun is involved in the migration and invasion induced by NUAK1, we performed transwell migration and invasion assay. As shown in Fig. 5E, silencing c-Jun remarkably reduced the numbers of migrated and invaded cells induced by NUAK1. Subsequently, we

examined whether overexpression of c-Jun attenuates the inhibitory effects of NUAK1 shRNA on Slug expression. The results showed that forced overexpression of c-Jun drastically rescued the expression and promoter activity of Slug mediated by NUAK1 shRNA (Fig. 5F, G). As expected, the migration and invasion of NUAK1-depleted KYSE30 cells were obviously enhanced by c-Jun overexpression (Fig. 5H). These findings together indicate that NUAK1 promotes the transcription of Slug induced by c-Jun, and thus enhances ESCC cell migration and invasion.

#### NUAK1 activates the JNK/c-Jun pathway to derive slug-mediated migration and invasion in ESCC cells

It has been reported that phosphorylation of c-Jun at Ser73 protects c-Jun from ubiquitination and subsequent degradation to increase its transcriptional activity [26]. We, therefore, examined whether NUAK1 influences the phosphorylation of c-Jun using Western blotting. As expected, forced overexpression of NUAK1 attenuated the protein levels of c-Jun and p-c-Jun (Ser73) (Fig. 6A and Additional file 1: Fig. S2A). Conversely, the protein levels of total c-Jun and its phosphorylation at Ser73 was diminished in NUAK1-silenced ESCC cells (Fig. 6A and Additional file 1: Fig. S2A). Next, we sought to explore the molecular mechanism by which NUAK1 regulates the phosphorylation of c-Jun. Overwhelming evidence showed that Akt [7] and mitogen-activated protein kinases (MAPKs) [27–29] are all able to phosphorylate c-Jun at Ser73 sites, we therefore examined whether NUAK1 regulates the activity of these proteins. Western blot analysis showed that the protein levels of p-Akt (S473) and total Akt were not obviously changed by NUAK1 (Fig. 6B and Additional file 1: Fig. S2B). Next, we investigated whether the family members of MAPKs such as JNK, ERK and p38 are involved in the activation of c-Jun through phosphorylation. Western blot analysis showed that the protein level of p-JNK (T183/Y185) was obviously enhanced in NUAK1-overexpressing ESCC cells, whereas was abrogated in NUAK1-depleted

(See figure on next page.)

**Fig. 5** c-Jun is crucial for NUAK1-induced migration and invasion in ESCC cells. **A** The expression of Slug mRNA was detected using qRT-PCR analysis. **B** The promoter activity of Slug was analyzed using the luciferase assay in NUAK1-overexpressing or knockdown ESCC cells. **C** The expression of c-Jun and Slug was analyzed in NUAK1-overexpressing EC109 cells treated with c-Jun shRNA. Quantification of indicated protein levels of n = 3 independent biological experiments (right panel). **D** The promoter activity of Slug was analyzed using the luciferase assay in NUAK1-overexpressing EC109 cells treated with c-Jun shRNA. **E** Cell migration (left panel) and invasion (right panel) were analyzed in NUAK1-overexpressing EC109 cells treated with c-Jun shRNA. **F** The expression of c-Jun and Slug was analyzed in NUAK1-knockdown KYSE30 cells treated with c-Jun and control vector plasmids. Quantification of indicated protein levels of n = 3 independent biological experiments (right panel). **G** The promoter activity of Slug was analyzed using the luciferase assay in NUAK1-knockdown KYSE30 cells treated with c-Jun and control vector plasmids. **H** Cell migration (left panel) and invasion (right panel) were analyzed in NUAK1-knockdown KYSE30 cells treated with c-Jun and control plasmids. Error bars denote mean  $\pm$  SD. \* $P < 0.05$ ; \*\* $P < 0.01$ ; \*\*\* $P < 0.001$ .  $P$  value was calculated by Student's t-test (for **A** and **B**, left panel) or one-way ANOVA with post hoc intergroup comparison by the Tukey's test (for **A** and **B**, right panel; **D**, **E**, **G** and **H**)

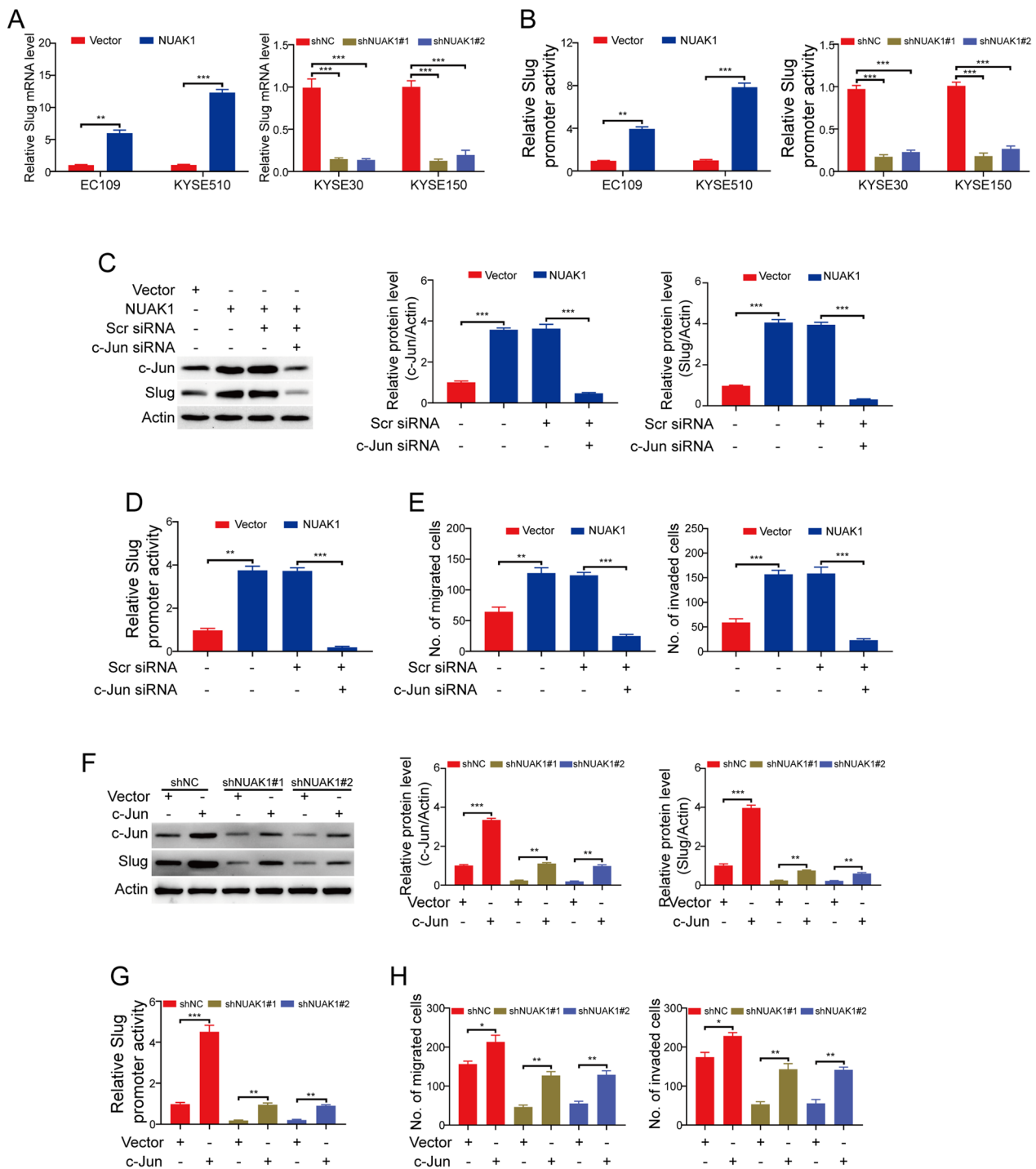


**Fig. 5** (See legend on previous page.)

KYSE30 and KYSE150 cells, compared with their control groups, respectively (Fig. 6C and Additional file 1: Fig. S2C). However, overexpression or knockdown of NUA1 has no considerable change in the levels of JNK, p-Erk (T202/Y204), Erk and p38 (Fig. 6C and Additional

file 1: Fig. S2C). The expression of p-p38 (T180/Y182) was upregulated in KYSE30 cells, but was downregulated in KYSE150 cells (Fig. 6C and Additional file 1: Fig. S2C). Furthermore, Co-IP assay also validated the interaction between NUA1 and JNK (Fig. 6D). To further

determine the role of JNK in NUA1-mediated upregulation of c-Jun in ESCC cells, NUA1-overexpressing EC109 cells were treated with two specific JNK inhibitors SP600125 and JNK-IN-8 for 24 h, and then the cell lysates were collected and subjected to Western blot analysis. As illustrated in Fig. 6E, pharmacological inactivation of JNK1/2 kinase by SP600125 and JNK-IN-8 remarkably diminished the expression of p-c-Jun (Ser73) and c-Jun. As expected, the protein and mRNA levels of Slug were also concomitantly inhibited (Fig. 6E, F). Consistently, luciferase reporter assay showed that the promoter luciferase activity of Slug in NUA1-overexpressing cells was obviously impaired by the two tested inhibitors of JNK (Fig. 6G). More importantly, pharmacological inhibition of JNK1/2 also significantly attenuated the migration and invasion of NUA1-overexpressing EC109 cells detected by transwell migration and invasion assay (Fig. 6H).

#### NUAK1 promotes tumor metastasis in nude mice

Considering that ectopic expression of NUA1 significantly enhanced the migration and invasion of ESCC cells in vitro, we then determined to further analyze the effect of NUA1 overexpression on tumor metastasis in vivo.  $1 \times 10^6$  EC109 cells were injected into BALB/c-nu/nu mice via the tail vein to establish a metastatic xenograft model and the tumor metastasis were examined after 8 weeks. As shown in Fig. 7A, mice injected with NUA1-EC109 cells formed more nodules on the lung surface than those injected with Vector-EC109 cells. To further confirm this conclusion, we injected KYSE30-shNUAK1 cells ( $1 \times 10^6$ ) into the nude mice via lateral tail vein and then examined the tumor metastasis after 8 weeks. The results showed that the number and size of metastatic nodules in the lungs was much smaller in NUA1-knockdown group than that of the control group (Fig. 7B). More importantly, IHC staining also showed that NUA1 promoted the levels of p-JNK (T183/Y185) and Slug in lung metastasis lesions derived from NUA1-overexpressing cells, compared with that of the control group (Fig. 7C). Vice versa, the expression of p-JNK (T183/Y185) and Slug in lung metastasis lesions was much lower in NUA1-knockdown cells than those

of cells transfected with shNC (Fig. 7D). Taken together, these data indicate that NUA1 promotes ESCC metastasis through JNK/c-Jun/Slug signaling pathway (Fig. 7E).

#### Discussion

In this study, our results showed that NUA1 was highly expressed in ESCC tissues but weakly expressed in paired normal esophageal epithelial specimens. Additionally, high NUA1 expression was positively associated with tumor tissue invasion, lymph node metastasis, poor pathological TNM stage and poor outcomes of patients with ESCC. These findings suggest that NUA1 is a potential diagnostic biomarker for ESCC patients. Loss- and gain-of-function studies demonstrated that expression of NUA1-targeting shRNA substantially suppressed ESCC cell EMT, migration and invasion in vitro and abrogated the metastatic behavior of ESCC cancer cells in xenograft models, indicating targeting NUA1 is a promising strategy for the treatment of ESCC patients.

As a serine/threonine kinase, NUA1 has been shown to play an oncogene in various human cancers. In colorectal cancer, depletion or inhibition of NUA1 renders human colorectal cancer cells and murine colorectal tumors vulnerable to oxidative stress-induced cell death [12]. Loss of NUA1 has recently been shown to trigger genomic instability and suppress tumor cell growth in pancreatic cancer [11]. Moreover, in epithelial ovarian cancer, NUA1 promotes cell adhesion, spheroid compaction and metastasis through regulation of fibronectin expression and matrix production [20]. Relevant to our own findings, an elevated NUA1 expression is positively associated with poor prognosis in ESCC patients. Interestingly, using gain- and loss-of function studies, we demonstrated that NUA1 hardly influences ESCC cell growth and colony formation, but greatly promotes EMT, migration, invasion and metastasis. Our findings were in agreement with a previous report, which showed that knockdown of NUA1 expression remarkably suppresses gastric cancer cell invasion and metastasis via regulating EMT, rather than proliferation in vitro and in vivo [18]. Altogether, those results from us and others suggest that

(See figure on next page.)

**Fig. 6** NUA1 activates the JNK/c-Jun pathway to derive Slug-mediated migration and invasion in ESCC cells. **A–C** Western blot analysis of p-c-Jun (S73) and c-Jun (**A**), p-Akt (S473) and Akt (**B**), p-JNK (T183/Y185), JNK, p-Erk (T202/Y204), Erk, p-p38 (T180/Y182) and p38 (**C**) in NUA1-overexpressing EC109 and KYSE510 cells, NUA1-knockdown KYSE30 and KYSE150 cells and control cells. **D** KYSE30 cell lysates were subjected to immunoprecipitation with IgG, anti-NUAK1 (left panel) or anti-JNK (right panel) antibodies. Immunoprecipitates were blotted with indicated antibodies. **E** The expression of p-c-Jun (S73), c-Jun and Slug was analyzed in NUA1-overexpressing EC109 cells treated with SP600125 and JNK-IN-8. Quantification of indicated protein levels of  $n=3$  independent biological experiments (right panel). **G** The promoter activity of Slug was analyzed using the luciferase assay in NUA1-overexpressing EC109 cells treated with SP600125 and JNK-IN-8. **H**, Cell migration and invasion were analyzed in NUA1-overexpressing EC109 cells treated with SP600125 and JNK-IN-8. Error bars denote mean  $\pm$  SD.  $^{**}P < 0.01$ ;  $^{***}P < 0.001$ . *P* value was calculated by one-way ANOVA with post hoc intergroup comparison by the Tukey's test (for **F–H**)

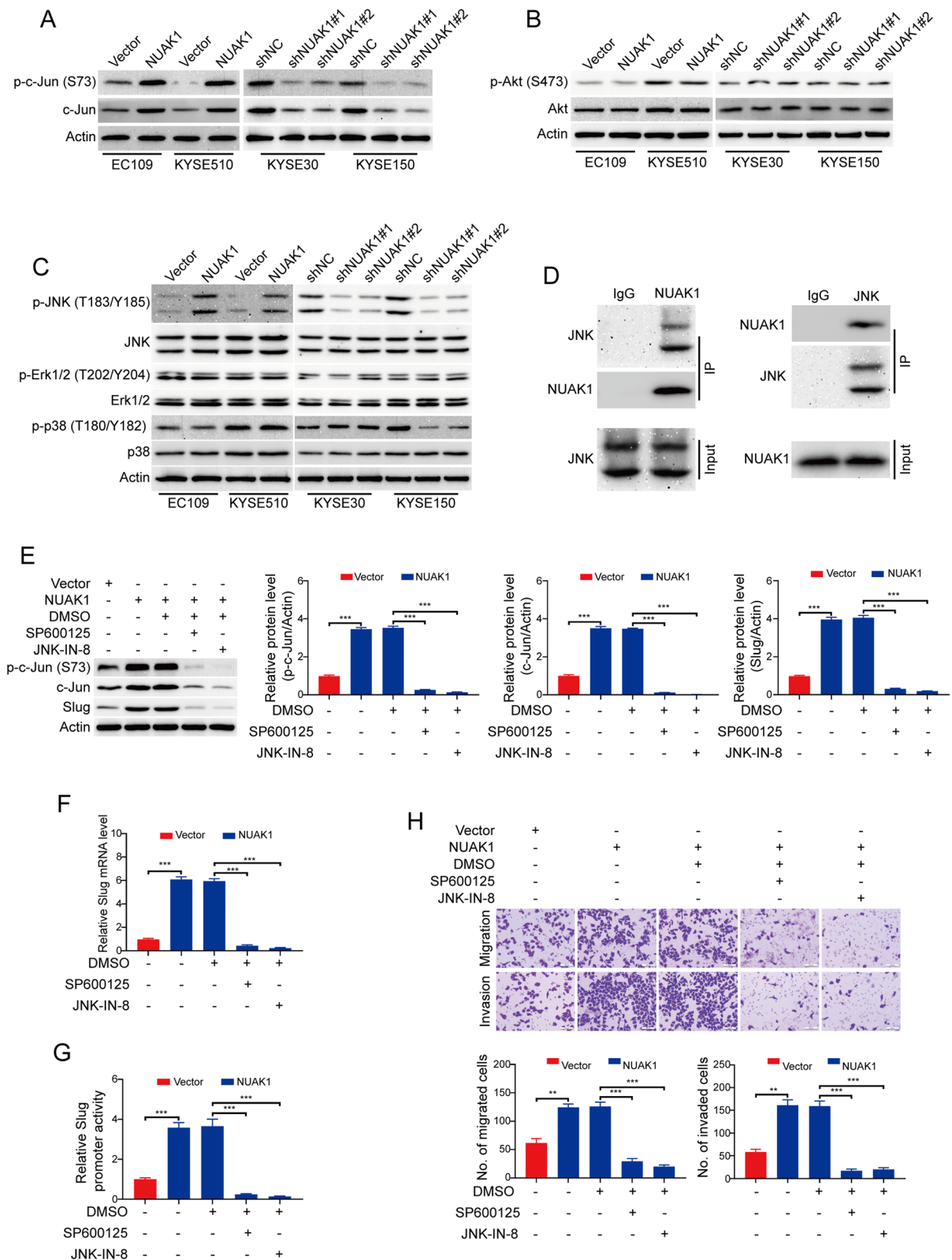


**Fig. 6** (See legend on previous page.)

targeting NUA1 is a promising strategy to treat metastatic malignancies.

EMT is a dynamic cellular process in which cells lose cell-cell junctions and baso-apical polarity and acquire mesenchymal features with increased motility and invasive potential [5]. In cancer, EMT has been associated with various tumor functions, including tumor initiation, malignant progression, migration, invasion and metastasis [5, 6]. As a family member of the snail, Slug has been described as a suppressive transcriptional factor of the epithelial marker E-cadherin and inducer of EMT and invasion [30–32]. Increased expression of Slug has been observed in several human cancers including ESCC [33], breast cancer [31], hepatocellular carcinoma [34] and gastric cancer [18]. In ESCC, the high Slug expression was associated with tumor tissue invasion, poor pathological stage and reduced disease free survival, and may serve as a diagnostic biomarker and as a predictor of poor disease prognosis for ESCC patients [33, 35]. Although several studies previously showed that high expression of NUA1 is positively associated with EMT, migration and invasion in gastric cancer [18], ovarian cancer [36], pancreatic cancer [37] and lung cancer [13], the underlying molecular mechanisms remain poorly understood. In this study, we demonstrated that NUA1 promoted ESCC cell EMT, migration and invasion at least in part through activating the transcription of Slug, which was based on the following facts: (1) Enforced expression of NUA1 drastically promoted the expression of Slug at both mRNA and protein levels. (2) In NUA1-over expressing cells, the knockdown of Slug abrogated tumor cell EMT, migration and invasion induced by NUA1. (3) Ectopic expression of Slug rescued the inhibitory effects of NUA1 shRNA on ESCC cell EMT, migration and invasion. Consistent with our findings in this study, a previous report has showed that knocking down NUA1 remarkably suppressed invasion and metastasis, as well as down-regulation of the mTOR/p70S6k signals, Slug and SIP1 in gastric cancer [18]. Together, these findings confirmed that EMT-related transcription factor Slug is critical for NUA1-mediated metastasis.

Emerging evidence suggests that JNK, a family member of mitogen-activated protein kinase (MAPK) signaling, regulates many physiological processes, including inflammatory responses, differentiation, cell proliferation, morphogenesis, survival and death [38]. In addition, it is increasingly apparent that JNK is also a key contributor to the cancer development and progression and plays a crucial role in several aspects of tumorigenesis, including cell differentiation, proliferation, invasion, angiogenesis, apoptosis, and metastasis [39]. In ESCC, the activation of the JNK signaling pathway has been described as a mediator of RAD18 to induce ESCC cell migration and invasion [40]. Consistent with these findings, in this study, we demonstrated a direct protein-protein interaction between NUA1 and JNK using Co-IP assay. We further found that NUA1 enhanced the phosphorylation of JNK and subsequently increased the transcription of Slug, whereas inhibiting JNK using two specific inhibitors, SP600125 and JNK-IN-8, remarkably abrogated NUA1-induced expression of Slug. In addition, both SP600125 and JNK-IN-8 were able to diminish the migration and invasion induced by NUA1 in tested ESCC cells. JNK was previously reported to induce c-Jun phosphorylation to enhance the binding of c-Jun to the promoters of oncogenes, thereby increasing its transcriptional activity [41]. Consistently, in this study, we found that treatment with JNK inhibitors in NUA1-overexpressing cells dramatically decreased the promoter activity of Slug induced by NUA1. Taken altogether, we confirmed that the highly elevated NUA1 promoted the migration, invasion and metastasis of ESCC cells by activating the JNK-Slug signaling pathway.

## Conclusions

In summary, our findings demonstrated that NUA1 promote ESCC cell migration, invasion and metastasis at least partly through activation of JNK/c-Jun/Slug signaling pathway. In addition, as depletion of NUA1 greatly inhibited the migration and invasion in vitro and metastasis in vivo, indicating targeting NUA1 is a promising therapeutic strategy for metastatic ESCC.

(See figure on next page.)

**Fig. 7** NUA1 promotes ESCC cell metastasis in nude mice. **A** Representative images of lung nodules formed by NUA1-overexpressing EC109 cells and control vector cells are shown. The numbers of lung metastatic nodules are shown in the right panel. *P* value was calculated by Student's *t*-test. **B** Left, representative images of lung tissues from animals bearing xenografts from KYSE30 cells with stable NUA1 knockdown. Right, the dot plots show the quantitative analysis of metastatic nodules on the lung surface in each group. *P* value was calculated by one-way ANOVA with post hoc intergroup comparison by the Tukey's test. **C** The expression of p-JNK (T183/Y185) and Slug was evaluated by IHC in lung tissues from EC109-NUA1 and vector cells. **D** Representative immunostaining of p-JNK (T183/Y185) and Slug in lung tissues from KYSE30-NUA1 shRNA and control shNC cells. Scale bars, 500  $\mu$ m. Error bars denote mean  $\pm$  SD. \*\*\**P* < 0.001. E, The working model of NUA1 in ESCC

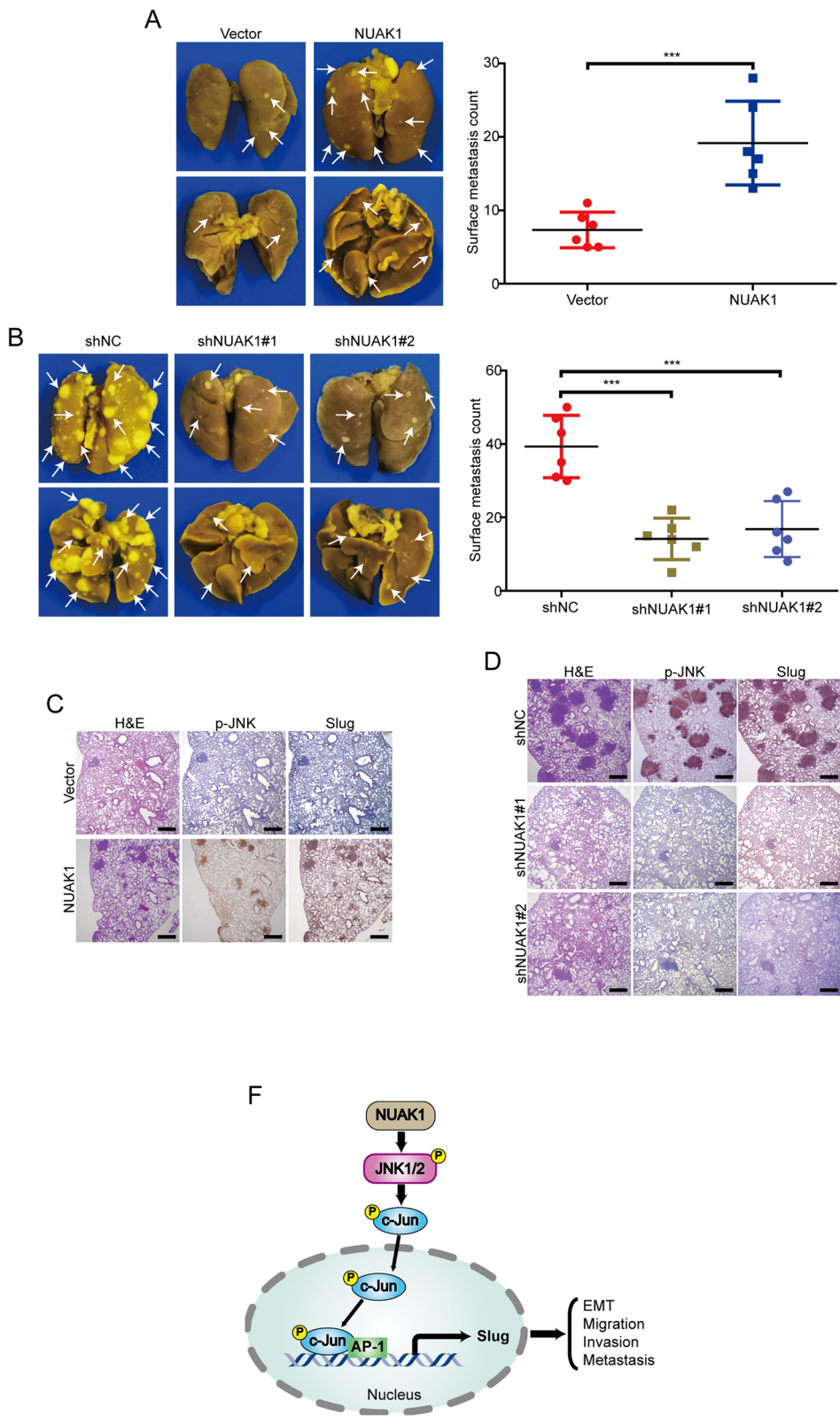


**Fig. 7** (See legend on previous page.)

## Supplementary Information

The online version contains supplementary material available at <https://doi.org/10.1186/s12935-023-03101-7>.

**Additional file 1: Figure S1.** NUAK1 promotes EMT via upregulation of Slug. **Figure S2.** NUAK1 activates the JNK/c-Jun pathway in ESCC cells. **Table S1.** Primers for qRT-PCR analysis. **Table S2.** Correlation between NUAK1 expression and clinicopathological parameters in 116 cases of ESCC.

### Acknowledgements

Not applicable.

### Author contributions

YHR and CL: data collection, statistical analysis, interpretation of results, and manuscript writing. WZ, SYF, DKX and YNN: data acquisition and statistical analysis. LH, LBB, HLL and XPF: statistical analysis and interpretation of results. CL, WCJ and XSQ: review, revision of the manuscript; material support, and study supervision. All co-authors have seen and approved this version of the manuscript.

### Funding

This work was supported by the National Natural Science Foundation of China (82103514 and 22104029), Project Funded by China Postdoctoral Science Foundation (2022M711050) and the Key Project of Science and Technology Research Funded by the Educational Commission of Henan Province (23A310021).

### Availability of data and materials

All data generated or analyzed during this study are included in this published article and its Additional files.

### Declarations

#### Ethics approval and consent to participate

This study was approved by the ethics committee of Henan University.

#### Consent for publication

Not applicable.

#### Competing interests

The authors declare no competing interests.

#### Author details

<sup>1</sup>School of Pharmacy, Henan University, N. Jinming Ave., Kaifeng 475004, Henan, China. <sup>2</sup>The Academy for Advanced Interdisciplinary Studies, Henan University, N. Jinming Ave., Kaifeng 475004, Henan, China. <sup>3</sup>The Key Laboratory of Natural Medicine and Immuno-Engineering, Henan University, N. Jinming Ave., Kaifeng 475004, Henan, China. <sup>4</sup>Department of Oncology, Huaihe Hospital of Henan University, Kaifeng 475004, Henan, China.

Received: 9 August 2023 Accepted: 16 October 2023

Published online: 02 November 2023

### References

- Sung H, Ferlay J, Siegel RL, Laversanne M, Soerjomataram I, Jemal A, et al. Global cancer statistics 2020: GLOBOCAN estimates of incidence and mortality worldwide for 36 cancers in 185 countries. *CA Cancer J Clin*. 2021;71:209–49.
- Zhang W, Luo J, Xiao Z, Zang Y, Li X, Zhou Y, et al. USP36 facilitates esophageal squamous carcinoma progression via stabilizing YAP. *Cell Death Dis*. 2022;13:1021.
- Hou S, Hao X, Li J, Weng S, Wang J, Zhao T, et al. TM4SF1 promotes esophageal squamous cell carcinoma metastasis by interacting with integrin alpha6. *Cell Death Dis*. 2022;13:609.
- Tian H, Lian R, Li Y, Liu C, Liang S, Li W, et al. AKT-induced lncRNA VAL promotes EMT-independent metastasis through diminishing Trim16-dependent vimentin degradation. *Nat Commun*. 2020;11:5127.
- Huang Y, Hong W, Wei X. The molecular mechanisms and therapeutic strategies of EMT in tumor progression and metastasis. *J Hematol Oncol*. 2022;15:129.
- Jinesh GG, Brohl AS. Classical epithelial–mesenchymal transition (EMT) and alternative cell death process-driven blebbistatin metastatic-witch (BMW) pathways to cancer metastasis. *Signal Transduct Target Ther*. 2022;7:296.
- Liu JH, Yang HL, Deng ST, Hu Z, Chen WF, Yan WW, et al. The small molecule chemical compound cinobufotalin attenuates resistance to DDP by inducing ENKUR expression to suppress MYH9-mediated c-Myc deubiquitination in lung adenocarcinoma. *Acta Pharmacol Sin*. 2022;43:2687–95.
- Suzuki A, Kusakai G, Kishimoto A, Lu J, Ogura T, Lavin MF, et al. Identification of a novel protein kinase mediating akt survival signaling to the ATM protein. *J Biol Chem*. 2003;278:48–53.
- Guan Y, Shi H, Xiao T. NUAK1 knockdown suppresses prostate cancer cell epithelial–mesenchymal transition, migration, and invasion through microRNA-30b-5p. *Int J Clin Exp Pathol*. 2018;11:5694–704.
- Liu J, Tang G, Huang H, Li H, Zhang P, Xu L. Expression level of NUAK1 in human nasopharyngeal carcinoma and its prognostic significance. *Eur Arch Otorhinolaryngol*. 2018;275:2563–73.
- Whyte D, Skalka G, Walsh P, Wilczynska A, Paul NR, Mitchell C, et al. NUAK1 governs centrosome replication in pancreatic cancer via MYPT1/PP1beta and GSK3beta-dependent regulation of PLK4. *Mol Oncol*. 2023;17:1212–27.
- Port J, Muthalagu N, Raja M, Ceteci F, Monteverde T, Kruspig B, et al. Colorectal tumors require NUAK1 for protection from oxidative stress. *Cancer Discov*. 2018;8:632–47.
- Chen P, Li K, Liang Y, Li L, Zhu X. High NUAK1 expression correlates with poor prognosis and involved in NSCLC cells migration and invasion. *Exp Lung Res*. 2013;39:9–17.
- Suzuki A, Lu J, Kusakai G, Kishimoto A, Ogura T, Esumi H. ARK5 is a tumor invasion-associated factor downstream of akt signaling. *Mol Cell Biol*. 2004;24:3526–35.
- Chang XZ, Yu J, Liu HY, Dong RH, Cao XC. ARK5 is associated with the invasive and metastatic potential of human breast cancer cells. *J Cancer Res Clin Oncol*. 2012;138:247–54.
- Obayashi M, Yoshida M, Tsunematsu T, Ogawa I, Sasahira T, Kuniyasu H, et al. microRNA-203 suppresses invasion and epithelial–mesenchymal transition induction via targeting NUAK1 in head and neck cancer. *Oncotarget*. 2016;7:8223–39.
- Yao CY, Gao ZX, Hou LL, Fang D. DKK1 promotes NUAK1 transcriptional expression through the activation akt in hepatocellular carcinoma. *Cell Biol Int*. 2023;47:383–93.
- Chen D, Liu G, Xu N, You X, Zhou H, Zhao X, et al. Knockdown of ARK5 expression suppresses invasion and metastasis of gastric cancer. *Cell Physiol Biochem*. 2017;42:1025–36.
- Lan X, Liu X. lncRNA SNHG1 functions as a ceRNA to antagonize the effect of miR-145a-5p on the down-regulation of NUAK1 in nasopharyngeal carcinoma cell. *J Cell Mol Med*. 2019;23:2351–61.
- Fritz JL, Collins O, Saxena P, Buensuceso A, Ramos Valdes Y, Francis KE, et al. A novel role for NUAK1 in promoting ovarian cancer metastasis through regulation of fibronectin production in spheroids. *Cancers (Basel)*. 2020;12:1250.
- Chen L, Bi S, Hou J, Zhao Z, Wang C, Xie S. Targeting p21-activated kinase 1 inhibits growth and metastasis via Raf1/MEK1/ERK signaling in esophageal squamous cell carcinoma cells. *Cell Commun Signal*. 2019;17:31.
- Zeng H, Yang H, Song Y, Fang D, Chen L, Zhao Z, et al. Transcriptional inhibition by CDK7/9 inhibitor SNS-032 suppresses tumor growth and metastasis in esophageal squamous cell carcinoma. *Cell Death Dis*. 2021;12:1048.
- Lin WH, Chang YW, Hong MX, Hsu TC, Lee KC, Lin C, et al. STAT3 phosphorylation at Ser727 and Tyr705 differentially regulates the EMT-MET switch and cancer metastasis. *Oncogene*. 2021;40:791–805.
- Zhang Y, Donaher JL, Das S, Li X, Reinhardt F, Krall JA, et al. Genome-wide CRISPR screen identifies PRC2 and KMT2D-COMPASS as regulators of distinct EMT trajectories that contribute differentially to metastasis. *Nat Cell Biol*. 2022;24:554–64.

25. Chen H, Zhu G, Li Y, Padia RN, Dong Z, Pan ZK, et al. Extracellular signal-regulated kinase signaling pathway regulates breast cancer cell migration by maintaining slug expression. *Cancer Res.* 2009;69:9228–35.
26. Fuchs SY, Dolan L, Davis RJ, Ronai Z. Phosphorylation-dependent targeting of c-Jun ubiquitination by Jun N-kinase. *Oncogene.* 1996;13:1531–5.
27. Wang Y, Zhou X, Lei Y, Chu Y, Yu X, Tong Q, et al. NNMT contributes to high metastasis of triple negative breast cancer by enhancing PP2A/MEK/ERK/c-Jun/ABCA1 pathway mediated membrane fluidity. *Cancer Lett.* 2022;547: 215884.
28. Zhang Y, Jiang K, Xie G, Ding J, Peng S, Liu X, et al. FGF21 impedes peripheral myelin development by stimulating p38 MAPK/c-Jun axis. *J Cell Physiol.* 2021;236:1345–61.
29. Waudby CA, Alvarez-Teijeiro S, Josue Ruiz E, Suppinger S, Pinotsis N, Brown PR, et al. An intrinsic temporal order of c-JUN N-terminal phosphorylation regulates its activity by orchestrating co-factor recruitment. *Nat Commun.* 2022;13:6133.
30. Liang Y, Cen J, Huang Y, Fang Y, Wang Y, Shu G, et al. CircNTNG1 inhibits renal cell carcinoma progression via HOXA5-mediated epigenetic silencing of slug. *Mol Cancer.* 2022;21:224.
31. Li W, Shen M, Jiang YZ, Zhang R, Zheng H, Wei Y, et al. Deubiquitinase USP20 promotes breast cancer metastasis by stabilizing SNAI2. *Genes Dev.* 2020;34:1310–5.
32. Zhang J, Fan X, Zhou Y, Chen L, Rao H. The PRMT5-LSD1 axis confers slug dual transcriptional activities and promotes breast cancer progression. *J Exp Clin Cancer Res.* 2022;41:191.
33. Hasan MR, Sharma R, Saraya A, Chattopadhyay TK, DattaGupta S, Walfish PG, et al. Slug is a predictor of poor prognosis in esophageal squamous cell carcinoma patients. *PLoS ONE.* 2013;8: e82846.
34. Meng J, Ai X, Lei Y, Zhong W, Qian B, Qiao K, et al. USP5 promotes epithelial–mesenchymal transition by stabilizing SLUG in hepatocellular carcinoma. *Theranostics.* 2019;9:573–87.
35. Uchikado Y, Natsugoe S, Okumura H, Setoyama T, Matsumoto M, Ishigami S, et al. Slug expression in the E-cadherin preserved tumors is related to prognosis in patients with esophageal squamous cell carcinoma. *Clin Cancer Res.* 2005;11:1174–80.
36. Zhang HY, Li JH, Li G, Wang SR. Activation of ARK5/miR-1181/HOXA10 axis promotes epithelial–mesenchymal transition in ovarian cancer. *Oncol Rep.* 2015;34:1193–202.
37. Huang X, Lv W, Zhang JH, Lu DL. miR-96 functions as a tumor suppressor gene by targeting NUA1 in pancreatic cancer. *Int J Mol Med.* 2014;34:1599–605.
38. Bubic C, Papa S. JNK signalling in cancer: in need of new, smarter therapeutic targets. *Br J Pharmacol.* 2014;171:24–37.
39. Anjum J, Mitra S, Das R, Alam R, Mojumder A, Emran TB, et al. A renewed concept on the MAPK signaling pathway in cancers: polyphenols as a choice of therapeutics. *Pharmacol Res.* 2022;184: 106398.
40. Zou S, Yang J, Guo J, Su Y, He C, Wu J, et al. RAD18 promotes the migration and invasion of esophageal squamous cell cancer via the JNK-MMPs pathway. *Cancer Lett.* 2018;417:65–74.
41. Zhang D, Jiang Q, Ge X, Shi Y, Ye T, Mi Y, et al. RHOV promotes lung adenocarcinoma cell growth and Metastasis through JNK/c-Jun pathway. *Int J Biol Sci.* 2021;17:2622–32.

## Publisher's Note

Springer Nature remains neutral with regard to jurisdictional claims in published maps and institutional affiliations.

Ready to submit your research? Choose BMC and benefit from:

- fast, convenient online submission
- thorough peer review by experienced researchers in your field
- rapid publication on acceptance
- support for research data, including large and complex data types
- gold Open Access which fosters wider collaboration and increased citations
- maximum visibility for your research: over 100M website views per year

At BMC, research is always in progress.

Learn more [biomedcentral.com/submissions](https://biomedcentral.com/submissions)

